

LASERS

https://doi.org/10.1070/QEL17427

Experimental technique for studying optical absorption in waveguide layers of semiconductor laser heterostructures

Yu.K. Bobretsova, D.A. Veselov, A.A. Podoskin, N.V. Voronkova, S.O. Slipchenko, M.A. Ladugin, T.A. Bagaev, A.A. Marmalyuk, N.A. Pikhtin

Abstract. **We report a technique for studying the absorption of optical radiation in layers of a semiconductor heterostructure by the method of probe radiation coupling. The studies are carried out using specially made isotype samples based on AlGaAs/GaAs, simulating an n-type doped laser waveguide with a concentration of 10^{17}–10^{18} cm^{-3}. The main features of the experimental setup and calculation methods are described. A high (up to 95%) efficiency of light coupling into the waveguide and an error in measuring the absorption coefficient at a level of 0.1 cm^{-1} are achieved. The possibilities of studying the polarisation and temperature dependences of radiation absorption by free carriers are experimentally demonstrated. It is shown that with an increase in temperature in the range 25–85°C, the absorption in the samples increases by 15%.**

Keywords: *semiconductor laser, semiconductor heterostructure, optical absorption by free carriers.*

1. Introduction

High-power semiconductor lasers of near-IR range have been developed and studied for more than half a century. Due to their unique properties (in the first place, high optical power and efficiency, as well as compactness), they have long established themselves as efficient sources of laser radiation. Nevertheless, there is still significant potential for improving their performance, which is partly related to advances in laser technology, but the main limiting factors lie in the field of fundamental physics. Thus, the maximum radiation power is currently limited by a decrease in the electro-optical conversion efficiency of the laser at high levels of current and temperature.

The saturation of the output power at high pump levels and temperatures is associated with several basic physical mechanisms. These are the transport of charge carriers in lightly doped waveguide layers, a decrease in the injection efficiency and internal quantum efficiency at high injection current densities, the finite time of carrier capture into the quantum well and energy relaxation, optical nonlinear effects in a laser cavity, and a number of others mechanisms [1–4]. In high-power pulsed semiconductor lasers, mechanisms dominate that cause a gradual increase in the concentration of charge carriers in the waveguide layers with an increase in the current density [5, 6]. The charge carriers in the waveguide recombine both radiatively and nonradiatively, which reduces the internal quantum efficiency of the laser, but the greatest contribution to a decrease in the laser power and efficiency is due to the absorption of laser radiation by free charge carriers.

The absorption of light by free carriers is a process of photon absorption, accompanied by an intraband transition of an electron or hole into an excited state. By virtue of the law of momentum conservation, transitions within one band are possible only when interacting with a third particle (phonon, impurity) [7]. The dependence of the absorption coefficient on the concentration of charge carriers can be both linear (for lightly doped semiconductors) and quadratic (for heavily doped semiconductors). As a rule, for semiconductor lasers with their lightly doped waveguides, it is common [7] to consider a linear dependence. In this case, absorption by free carriers is described by the absorption cross-section parameter σ, which relates the absorption coefficient α and the concentration of charge carriers:

$$\alpha = \sigma_n n + \sigma_p p, \tag{1}$$

where n and p are the concentrations of electrons and holes; and σ_n and σ_p are their absorption cross sections.

In the most authoritative works devoted to lasers based on InGaAs/AlGaAs/GaAs, absorption cross sections for electrons and holes in GaAs are used, equal to 4×10^{-18} cm^2 and 12×10^{-18} cm^2 [1–3] or 3×10^{-18} cm^2 and 10×10^{-18} cm^2 [8–10], respectively. However, other values of the absorption cross sections are also encountered in the literature, and their scatter is quite large. Thus, in [7, 11, 12] $\sigma_n = 3 \times 10^{-18}$ cm^2 and $\sigma_p = 7 \times 10^{-18}$ cm^2 are used. According to the data of Ref. [13], it is possible to determine the electron absorption cross section at a temperature of 297 K and a concentration of 4.9×10^{17} cm^{-3} as $\sigma_n = 3.5 \times 10^{-18}$ cm^2. The absorption cross section of holes in p-GaAs experimentally measured in [14] at room temperature is about 8.5×10^{-18} cm^2 (at a concentration of holes of 1.5×10^{18} cm^{-3}), and the value calculated theoretically [15] is 6×10^{-18} cm^2 (for concentrations 10^{14}–10^{18} cm^{-3}). The absorption cross sections calculated in [16] for nonequilibrium charge carriers $\sigma_n = 1.05 \times 10^{-18}$ cm^2 and $\sigma_p = 1.55 \times 10^{-19}$ cm^2 differ significantly from the generally accepted ones; however, these values agree with the data of Ref. [17].

In addition to the indicated scatter of σ_n and σ_p values, we note a significant dependence of absorption by free carriers on various factors. The spectral dependence of the absorption coefficient is qualitatively known, but it is difficult to describe

Yu.K. Bobretsova, D.A. Veselov, A.A. Podoskin, N.V. Voronkova, S.O. Slipchenko, N.A. Pikhtin Ioffe Institute, Politekhnicheskaya ul. 26, 194021 St. Petersburg, Russia; e-mail: nike@hpld.ioffe.ru;
M.A. Ladugin, T.A. Bagaev, A.A. Marmalyuk JSC 'Polyus Research Institute of M.F. Stelmakh', ul. Vvedenskogo 3, korpus 1, 117342 Moscow, Russia

Received 31 August 2020
Kvantovaya Elektronika **51** (2) 124–128 (2021)
Translated by V.L. Derbov

it quantitatively. For example, in [7] absorption is considered to be a power function of the photon wavelength, and the power depends on the type of particles involved in this process. Experimental data on the spectral dependence of the absorption coefficient are given in [13, 14], theoretical calculations are given in [15]. In the same papers, one can find the temperature dependences of absorption by free carriers. The absorption coefficient for n-GaAs increases by about a factor of 1.5 with a change in temperature from 100 to 443 K [13], and for p-GaAs it grows by 40% with an increase in temperature from 295 to 370 K [14]. All the data presented refer to GaAs, while for AlGaAs they are practically absent. In practice, however, semiconductor laser waveguides are usually made of AlGaAs, often with a high aluminium content. The calculated dependences of absorption on the aluminum content in the material for a wavelength of 808 nm, presented in [18], demonstrate a noticeable increase in absorption with an increase in the Al fraction (hole concentration $p = 2.5 \times 10^{17}$ cm^{-3}).

Thus, most studies of absorption by free carriers in semiconductors are of a fundamental nature, applicable for a general description of processes with an accuracy of an order of magnitude, and are performed for an excessively wide range of conditions. In this regard, as applied to high-power semiconductor lasers operating at wavelengths of 800–1100 nm, studies of the absorption coefficient in the mid-IR and far-IR regions and for three to four temperatures in the range 100–443 K provide little useful information. Some of the experimental work was carried out more than half a century ago [13, 17]. It is obvious that since then the semiconductor technology has changed significantly, the quality of heterostructures has dramatically improved, which could not but affect the absorption cross section. Modern mathematical analysis of the operation of high-power semiconductor lasers requires more and more accurate parameters for calculation, and the absorption cross sections on free carriers are one of the key factors determining the reliability of the results. Thus, for the development of semiconductor lasers, it is necessary to continue studies of absorption of radiation on free carriers in order to obtain more accurate and reliable values for modern systems of materials.

We propose a new technique for studying optical absorption, based on the method of coupling probe radiation into a sample with an optical waveguide [6, 19, 20]. This technique should make it possible to study absorption in different materials at different parameters (radiation wavelength, temperature, dopant concentration). The main goal of this work was to create such an experimental technique for measuring absorption by free carriers, which would allow studying this process as applied to the specifics of heterostructures of high-power lasers.

Expression (1) is valid for uniform illumination of the layer under study. In waveguide structures, the distribution of electromagnetic radiation, which experiences optical losses, is determined by the mode structure; therefore, Eqn (1), e. g., for electrons takes the following form:

$$\alpha = \sigma_n \int n(x)\psi^2(x)\mathrm{d}x, \qquad (2)$$

where $\psi(x)$ is the intensity distribution of the fundamental waveguide mode; and $n(x)$ is the distribution of the electron concentration along the transverse horizontal x axis [21]. Thus, in order to determine the absorption cross section from the experimental data, it is necessary to know both the total absorption coefficient and the concentration and optical field distributions. The concentration distribution is determined by the doping profile formed during the growth of the heterostructure, and the mode shape is determined by the composition and thickness of the layers. The main task of this work is to create a technique for measuring the absorption coefficient. Calculation of absorption cross sections requires additional measurements of doping profiles and analysis of waveguide modes, which will be done in a separate work. Here we present the results of the development of the research methodology, specific features of the construction and operation of the experimental setup, as well as the first results of measurements.

2. Experimental samples

For the experiment, special samples based on AlGaAs/GaAs were fabricated to simulate a laser waveguide. The heterostructure of the samples was grown by MOCVD in a technological cycle similar to the cycle for laser heterostructures on a GaAs substrate and included an $Al_{0.1}Ga_{0.9}As$ waveguide 3 μm thick between $Al_{0.27}Ga_{0.73}As$ emitters 2 μm thick, as well as GaAs buffer and contact layers. In contrast to a conventional laser heterostructure, the experimental one has no p–n junction and active region. To study absorption by electrons, the entire structure is isotypically doped with silicon with a concentration $n = 10^{17}–10^{18}$ cm^{-3}. This doping level is most convenient from the point of view of the technique for studying the absorption cross section. It is also interesting from a practical point of view, since it approximately corresponds to the average value of the nonequilibrium concentration of charge carriers, which is accumulated in the waveguide during operation of a semiconductor laser at high current densities [5].

To achieve the best localisation of the wave in the layer with the material under study and to simplify the coupling of the probe light into the structure, a thick (3 μm) $Al_{0.1}Ga_{0.9}As$ waveguide was chosen. It should be noted that lasers with waveguides of exactly this thickness and composition were studied in our papers [6, 20]. Cladding layers 2 μm thick provide optical confinement and prevent the propagation of the entering radiation outside the waveguide. In accordance with the calculation data for the mode distribution of the electromagnetic field in the heterostructure, the fraction of radiation propagating inside the waveguide is at least 99%. The contact layer was grown to implement thermal contact and the possibility of soldering the samples onto the carriers using standard technology.

The grown heterostructure (in comparison with standard laser structures) underwent a simplified cycle of postgrowth processing, which included the thinning of the plate and the formation of contact from the side of the layers. The experimental samples have neither mesa grooves that form a laser strip, nor a dielectric coating on the passive parts and a contact layer on the side of the substrate.

Sets of crystal samples of a given length and width were obtained by cleaving a heterostructure plate. The mirrors of all samples were formed by cleaving, and no antireflection or reflective coatings were applied. Each chip was mounted on a carrier, layers down.

3. Research technique

The experimental setup is schematically shown in Fig. 1. The source of probe radiation was a single-mode laser diode (*1*) with a radiation wavelength of 1063 nm and a spectral width

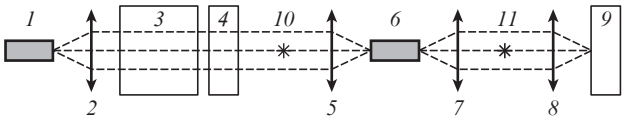

Figure 1. Optical scheme of the setup for studying the absorption coefficient: (*1*) probe laser; (*2*, *5*, *7*) aspherical lenses; (3) optical isolator; (*4*) half-wave phase plate; (*6*) test sample; (*8*) lens; (*9*) CMOS matrix; (*10*, *11*) points at which the power was measured.

of less than 2 nm at half maximum. The probe radiation is not affected by interband absorption in the material under study, but is absorbed by free charge carriers, heterostructure heterogeneities and its interfaces. Thus, the absorption in the sample under study is similar to the absorption of intrinsic radiation in a laser. The probe radiation was coupled into the end of the waveguide of a sample 6 by means of an optical system consisting of Thorlabs aspherical lenses (*2*) and (*5*) with a numerical aperture of 0.3–0.5 and type C antireflection coating (reflection coefficient less than 0.5% in the range 1050–1700 nm). In more detail, the radiation coupling into the sample is shown in Fig. 2. To suppress the back reflection of the probe radiation, an optical isolator (*3*) was used, at the output of which the radiation was linearly polarised. A half-wave phase plate (*4*) served to rotate the plane of polarisation when studying the effect of polarisation on absorption in the sample. At the exit of the sample, the probe radiation was collimated by an aspherical lens (*7*) and, with the help of an objective lens (*8*), was focused on a CMOS matrix (*9*). The resulting image of the transmitted radiation helped to align the setup, but the matrix was used only as an auxiliary tool. The primary data for calculating the absorption were the input and output power values, which were measured with a Thorlabs S146C bolometer. The control of the probing radiation power before each measurement was carried out at point *10* (Fig. 1), the power value was ensured with a given degree of accuracy. After completing the alignment of the scheme, the bolometer was placed at point *11* to determine the power of the transmitted radiation.

To ensure the accuracy and stability of the optical scheme, the laboratory stand was placed on an optical table with vibration-isolating pneumatic supports. The laser and sample temperature control system containing Peltier elements and temperature sensors ensured temperature stability with an accuracy of 0.05 °C. For the probe laser, the temperature was kept constant and equal to 25 °C, and the temperature of the sample under study could be selected in the range of 25–85 °C. The probe radiation power was maintained at a level of 12 mW.

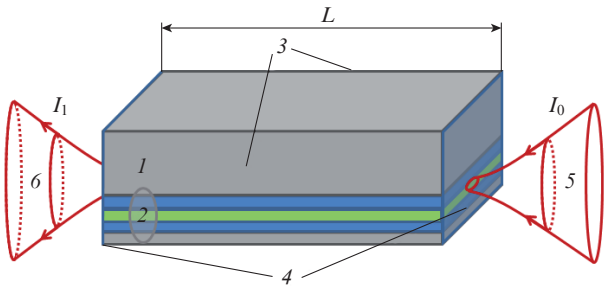

Figure 2. Schematic of the sample under study and radiation input into it: (*1*) substrate; (*2*) heterostructure; (*3*) lateral facets of the sample; (*4*) end facets of the sample; (*5*) probe radiation with power I_0; (*6*) radiation with power I_1 passed through the sample; L is the length of the sample.

A probe beam of constant power was in turn coupled into the waveguides of samples with different cavity lengths, at the output of which the optical power was measured. Using a set of output power values in samples of different lengths, the absorption inside the waveguide was calculated.

Consider this procedure in more detail. Let the samples (Fig. 2) of length L_1 and L_2 ($L_2 > L_1$) be studied and the corresponding output power levels be I_1 and I_2 (obviously, $I_1 > I_2$). If we do not take into account the re-reflection of the probe radiation inside the crystal from its ends that form a Fabry–Perot resonator, we can use the formula

$$\alpha = \frac{1}{L_2 - L_1} \ln \frac{I_1}{I_2}, \tag{3}$$

which is valid in the case of ideal antireflection coatings of the crystal facets. To minimise the uncertainty associated with the error in determining the reflection coefficients of dielectric coatings, when they cannot be neglected, we used another approach. For all the samples under study, the reflection coefficients of the cleaved facets are 30.2%; however, for an accurate calculation of the absorption, it is necessary to take into account the multiple passes of light through the cavity. Therefore, we used a system of two equations that takes into account five passages of radiation through samples of length L_1 and L_2:

$$\begin{aligned} I_1 &= I_0 \exp(-\alpha L_1)(1-R)^2 + I_0 \exp(-3\alpha L_1) R^2 (1-R)^2 \\ &\quad + I_0 \exp(-5\alpha L_1) R^4 (1-R)^2, \\ I_2 &= I_0 \exp(-\alpha L_2)(1-R)^2 + I_0 \exp(-3\alpha L_2) R^2 (1-R)^2 \\ &\quad + I_0 \exp(-5\alpha L_2) R^4 (1-R)^2, \end{aligned} \tag{4}$$

where I_0 is the power of the probe radiation at the input to the sample; R is the reflectance of the mirrors. System (4) is solved with respect to unknowns α and I_0. The main purpose of the calculation is the absorption coefficient α; however, the possibility of determining the value of the input power is also important from a technical point of view. The ratio of the measured power of light coupled into the crystal to the calculated value I_0 gives the efficiency of coupling light into the laser waveguide. Providing a high value of this coefficient ensures the reliability of the measurement results.

In the system of Eqns (4), the divergence of the probe radiation along the transverse x axis (in the plane of the heterostructure layers) is not taken into account, since it does not exceed 3° inside the crystal; however, the radiation that passes the total distance $5L$ inside the crystal, at which the radiation spot has time to increase significantly is taken into account. If the transverse size of the radiation exceeds the width of the crystal, it will begin to be reflected from the side walls, which can potentially reduce the output power from long samples and, therefore, affect the measurement results. To avoid this, for each crystal length, its minimum permissible width was calculated so that after five passes of the cavity the size of the

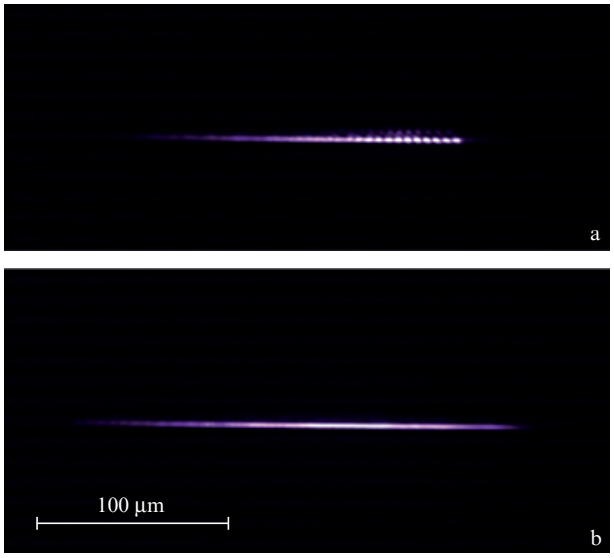

Figure 3. Images of radiation transmitted through a 1760 μm long sample when the input beam hits the edge of the sample (a) and the centre of its end facet (b).

output spot remained smaller than the crystal width. The absence of reflections from lateral facets during sample alignment was monitored using a CMOS camera. In the image of the transmitted probe radiation, the presence of rays reflected from the lateral edges manifested itself in the form of a characteristic interference pattern (Fig. 3a). The image of radiation transmitted without multiple reflections (Fig. 3b) is monotonic with a close-to-Gaussian transverse intensity distribution.

4. Experimental results and discussion

After adjusting the experimental setup and perfecting the measurement technique, we considered the effect of radiation polarisation on its transmission under the rotation of a half-wave phase plate and measuring the output power from samples of different lengths at temperatures of 25 and 85 °C. In all cases, the angle of rotation of the polarisation plane had little effect on the level of the output power, i.e. its change was comparable to the measurement error; therefore, the polarisation dependence of absorption was not studied in more detail. The phase plate was rotated so that in all further experiments the polarisation plane of the input radiation corresponded to the TE polarisation for the sample waveguide.

The radiation power was measured at the output of samples with lengths of 1230, 1760, and 5430 μm in the temperature range 25–85 °C. At least five samples of each length were used; the system was aligned for each sample and at each temperature. Thus, a set of power values was obtained for samples of different lengths L and widths W at different temperatures. For example, the average values of the measured powers and their spread for each length at 25 °C were as follows: 405.2 ± 5.4 μW for L = 5430 μm and W = 1500 μm, 2168.4 ± 30.5 μW for L = 1760 μm and W = 500 μm, and 2890 ± 9.8 μW for L = 1230 μm and W = 500 μm. In the subsequent calculations, only the average values of the powers were used (for samples of the same length at the same temperature), and their scatter was taken into account when estimating the errors.

Since the calculation using Eqn (4) is possible for a pair of samples of different lengths, and samples with three lengths were used, the calculations of the absorption coefficient were carried out for three pairs with lengths of 5430 and 1760 μm, 5430 and 1230 μm, 1760 and 1230 μm with a change in their temperature from 25 to 85 °C (Fig. 4). In principle, if we do not take into account the experimental errors, all three dependences shown in the figure should coincide. However, it can be seen that the values of the absorption coefficient obtained for pairs of 5430 and 1760 μm, 5430 and 1230 μm [curves (*1*) and (*2*)] are close, while the pair of the shortest samples [curve (*3*)] demonstrates noticeably larger both the magnitude and the spread of the values of the absorption coefficient. Thus, a small error in the case of measurements of a pair of samples with close lengths leads to a significant error in the calculation result. Therefore, the most preferable is the pair with the maximum difference of sample lengths [curve (*2*)]. It should be noted that for all pairs of samples, the temperature dependence of the absorption coefficient looks almost the same.

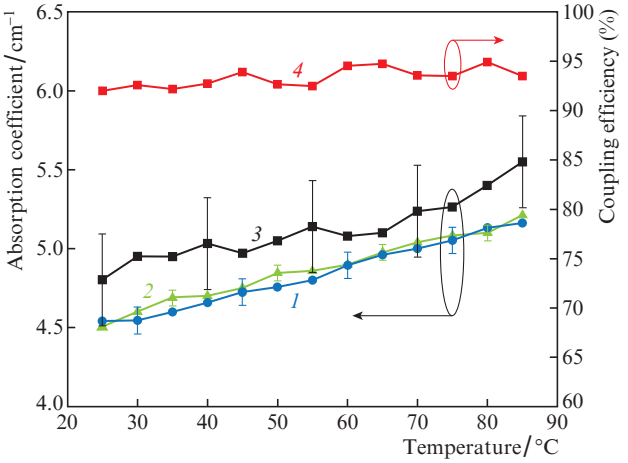

Figure 4. Temperature dependences of the absorption coefficient obtained for three pairs of samples with lengths of (*1*) 5430 and 1760 μm, (*2*) 5430 and 1230 μm, (*3*) 1760 and 1230 μm, as well as the radiation input coefficient for a pair with lengths of (*4*) 5430 and 1230 μm.

In addition to the measured absorption coefficients, Eqn (4) allows determining the efficiency of light coupling into the waveguide. To evaluate it, the power was measured at point *11* (see Fig. 1) without a sample. Lens *7* collimated radiation at the exit from lens *5* and directed it into the bolometer. The measured power I_m was 11.7 mW; it corresponds to the power entering the crystal, taking into account all losses on the lenses. The ratio of the power I_0, calculated using Eqn (4), to I_m gives a calculated coupling efficiency of 90%–95% in all cases, which, as can be seen from Fig. 4, for a pair of samples 5430 and 1230 μm [curve (*4*)] is practically independent of temperature. Note that such a high coupling efficiency was obtained due to careful calculations of the optical scheme, selection and alignment of lenses.

Let us estimate the error in the calculation results. It depends on all the input parameters of the calculation, including the error in determining the sample length and the reflection coefficient of the facets. The relative error in measuring the power for all samples and temperatures did not exceed 1.5%. The error in measuring the lengths of the samples is ± 10 μm, the relative error does not exceed 0.8%. It is more difficult to estimate the error in determining the reflectance of the mirror. In addition to possible inaccuracies in its calcula-

tion, one should take into account the effect of temperature on the refractive index and, therefore, on the reflection coefficient. According to our estimates, the absolute error of its determination does not exceed ± 3% with a reflection coefficient of 30.2% (relative error 10%). Let us illustrate the influence of the error in measuring the lengths of the samples and the reflection coefficients of the mirrors by the example of a pair with lengths of 5430 and 1230 μm, which provides the highest accuracy in determining the absorption coefficient. Variations in the lengths of the samples within ± 10 μm and the reflection coefficient within 27%–33% lead to a change in the calculated absorption coefficient not greater than 0.7% and 0.4%, respectively. The total maximum calculation error for a pair of samples with a maximum length difference did not exceed 1.2% (Fig. 4). Since our task was to ensure the accuracy of the measurement method at a level of 0.1 cm^{-1}, judging by the results of the analysis of errors, it can be considered fulfilled.

The absorption coefficient obtained in this work is determined by the doping profile and mode configuration. An analysis of the absorption cross section, taking into account the measured distribution of the dopant concentration, will be carried out in further studies.

Note that an increase in temperature leads to an increase in absorption in the layers: with a rise in temperature from 25 to 85°C, it increases by about 15%, which is in good agreement with the literature data [13].

In conclusion, we emphasise that the proposed technique for studying the absorption of optical radiation in heterostructures is quite accurate, informative, and has a significant potential for applications. Given samples of different compositions, with different levels and types of doping, it is possible to study the effect of these parameters, as well as technological factors of epitaxial growth on the absorption of radiation by free carriers. The technique allows studying the temperature and polarisation, as well as, in principle, the spectral dependences of the absorption coefficient. In the latter case, it is necessary to use either a set of single-mode lasers with different wavelengths, or a tunable source of coherent radiation.

In the future, we plan to prepare a series of heterostructures with different compositions of the waveguide material and dopant concentrations, accurately measure the doping profile of each heterostructure and conduct studies of the absorption coefficient using the developed technique.

Acknowledgements. Studies of the epitaxial growth of heterostructures were supported by the Russian Science Foundation (Project No. 19-79-30072); experimental studies were supported by the Russian Foundation for Basic Research (Grant No. 19-32- 90070).

References

1. Piprek J. *Opt. Quantum Electron.*, **51** (60), 10 (2019).
2. Wenzel H., Crump P., Pietrzak A., Wang X., Erbert G., Tränkle G. *New J. Phys.*, **12**, 085007 (2010).
3. Dogan M., Michael C.P., Zheng Y., Zhu L., Jacob J.H. *Proc. SPIE*, **8965**, 89650P (2014).
4. Soboleva O.S., Zolotarev V.V., Golovin V.S., Slipchenko S.O., Pikhtin N.A. *Transact. Electron. Devices*, in press.
5. Piprek J., Li Z.M. *IEEE Photonics Technol. Lett.*, **30** (10), 963 (2018).
6. Veselov D.A., Bobretsova Yu.K., Leshko A.Y., Shamakhov V.V., Slipchenko S.O., Pikhtin N.A. *J. Appl. Phys.*, **126**, 213107 (2019).
7. Pikhtin N.A., Slipchenko S.O., Sokolova Z.N., Tarasov I.S. *Semiconductors*, **38** (3), 360 (2004) [*Fiz. Tekh. Poluprovodn.*, **38** (3), 374 (2004)].
8. Ryvkin B., Avrutin E. *Electron. Lett.*, **42** (22), 1283 (2006).
9. Ryvkin B., Avrutin E. *Semicond. Sci. Technol.*, **32** (1), 015004 (2017).
10. Ryvkin B., Avrutin E. *2006 Intern. Conf. Transp. Opt. Networks*, **2**, 246 (2006).
11. Erbert G., Bugge F., Fricke J., Ressel P., Staske R., Sumpf B., Wenzel H., Weyers M., Tränkle G. *IEEE J. Select. Top. Quantum Electron.*, **11** (5), 1217 (2005).
12. Casey H., Panish M.B. *Heterostructure Lasers* (New York: Academic Press, 1978; Moscow: Mir, 1981).
13. Spitzer W.G., Whelan J.M. *Phys. Rev.*, **114** (1), 59 (1959).
14. Ryvkin B., Georgievsky A. *Semiconductors*, **33** (7), 813 (1999) [*Fiz. Tekh. Poluprovodn.*, **33** (7), 887 (1999)].
15. Krishnamurthy S., Yu Z.G., Gonzalez L.P., Guha Sh. *J. Appl. Phys.*, **109** (3), 033102 (2011).
16. Rozhkov A.V. *Semiconductors*, **54** (8), 869 (2020) [*Fiz. Tekh. Poluprovodn.*, **54** (8), 721 (2020)].
17. Fan H.Y. *Semicond. Semimet.*, **3**, 405 (1967).
18. Bulashevich K.A., Mymrin V.F., Karpov S.Yu., Demidov D.M., Ter-Martirosyan A.L. *Semicond. Sci. Technol.*, **22**, 502 (2007).
19. Veselov D.A., Pikhtin N.A., Lyutetsky A.V., Nikolaev D.N., Slipchenko S.O., Sokolova Z.N., Shamakhov V.V., Shashkin I.S., Kapitonov V A.A., Tarasov I.S. *Quantum Electron.*, **45** (7), 597 (2015) [*Kvantovaya Elektron.*, **45** (7), 597 (2015)].
20. Gavrina P.S., Soboleva O.S., Podoskin A.A., Kazakova A.E., Kapitonov V.A., Slipchenko S.O., Pikhtin N.A. *Semiconductors*, **54** (8), 882, (2020) [*Fiz. Tekh. Poluprovodn.*, **54** (8), 734 (2020)].
21. Ryvkin B.S., Avrutin E.A. *J. Appl. Phys.*, **97**, 123103 (2005).